

Title	Studies on the Mechanical Characteristics of the Orthotropic Plywood Shallow Shells (I) : Numerical Analysis
Author(s)	MASUDA, Minoru; MAKU, Takamaro
Citation	Wood research : bulletin of the Wood Research Institute Kyoto University (1972), 52: 44-71
Issue Date	1972-01-31
URL	<a href="http://hdl.handle.net/2433/53415">http://hdl.handle.net/2433/53415</a>
Right	
Type	Departmental Bulletin Paper
Textversion	publisher

# Studies on the Mechanical Characteristics of the Orthotropic Plywood Shallow Shells (I)\*

—Numerical Analysis—

MINORU MASUDA\*\* and TAKAMARO MAKU\*\*

**Abstract**—It is proved that the coefficients  $B_{ij}$  and  $D_{ij}$  of the fundamental equations of the layered orthotropic shells can be calculated from the measured moduli of elasticity ( $E_{Xc}, E_{Yc}, \dots$ ) and ( $E_{Xb}, E_{Yb}, \dots$ ), respectively, according to the procedure shown in (3-17) and (3-18). And this is better than the calculation using the elastic constants of veneers, because the former include the effects of the adhesion and the pressing.

It is very difficult to solve precisely the fundamental equations when the axes of elastic symmetry do not coincide with those of coordinates ( $B_{16} \neq 0, B_{26} \neq 0, D_{16} \neq 0$  or  $D_{26} \neq 0$ ). The authors attempted to solve them by the application of the finite difference method and succeeded in solving them with good accuracy of the approximation (see Figs. 7, 8 and 9). The application to the layered orthotropic shells is more complicated than that to the isotropic shells, so the unique techniques were needed.

The characteristics of the layered orthotropic shallow shells with roller-supported edges were made clear by this numerical analysis, that is to say, the influence of the following problems were analysed, and the results are shown in the figures and the tables; 1) the curvature, 2) the shape of the shells (H. P., Cyl., E. P.), 3) ratio of the side lengths, 4) the moduli of elasticity, 5) the direction of the elastic principal axis, 6) uniform pressure and a concentrated load.

## Introduction

Theoretical studies on the mechanical characteristics of layered orthotropic shells are very important to make clear the mechanical characteristics of plywood shell roofs<sup>1,2)</sup> (include sandwich construction) and furniture made of curved plywood. But it is very difficult to get mathematically exact solution of the fundamental equations of layered orthotropic shells, so an approximate method of the solution must be used. As the approximate methods, finite difference method, finite element methods and Ritz-Galerkin's method are considered to be applicable. In the present paper, applications of the finite difference methods are attempted to the problems of layered orthotropic shallow shells with four edges roller supported, and the solutions with good approximate accuracy are obtained.

---

\* Presented at the 20th Meeting of the Japan Wood Research Society, Tokyo, Sep. 1970.

\*\* Division of Composite Wood.

Table 1. List of symbols used.

Symbol	Definition
$C$	elastic constant
$E$	modulus of elasticity
$G$	modulus of rigidity
$I$	moment of inertia
$M$	bending moment
$N$	membrane stress
$Q$	shearing force
$X, Y$	axes of elastic symmetry
$a, b$	shell dimensions in $x$ and $y$ directions, respectively
$d$	mesh size of the finite difference method
$m$	number of the layers
$p$	applied pressure
$t$	thickness
$u, v$	components of displacement in $x$ and $y$ directions, respectively
$w$	deflection
$x, y$	rectangular coordinates or curvilinear coordinates
$z$	distance from the neutral plane of plates and shells
$\gamma$	shearing strain
$\epsilon$	strain
$\theta$	angle between $x$ axis and $X$ axis
$\mu$	Poisson's ratio
$\sigma$	normal stress
$\tau$	shearing stress
$b$ (subscript)	in bending of layered plates and shells
$c$ ( " " )	in compression or tension of layered plates and shells
$n$ ( " " )	in $n$ -th lamina or $n$ -th veneer
$x, y$ ( " " )	in $x$ and $y$ directions, respectively
$X, Y$ ( " " )	in $X$ and $Y$ directions, respectively

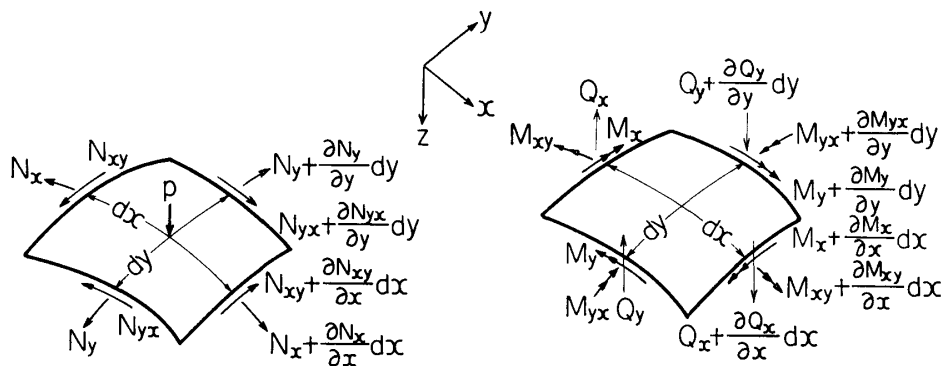
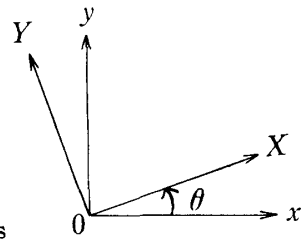


Fig. 1. Figures for the derivation of the equilibrium equations (1-3)~(1-7).

**Theory of Orthotropic Plywood Shallow Shells**

**1. The Fundamental Equations of Orthotropic Plywood Shallow Shells<sup>3-6)</sup>**

In this paper following assumptions are used for the theoretical analysis of orthotropic plywood shallow shells; 1) small and elastic deformation, 2) Navier's assumption, 3) symmetrical construction of lamination and perfect adhesion, 4) uniform thickness.

The fundamental equations are derived by the following procedure: The shapes of the shells are given by

$$f(x, y) = \frac{k_x}{2}x^2 + \frac{k_y}{2}y^2 + k_{xy}xy. \quad (1-1)$$

$k_x$ ,  $k_y$  and  $k_{xy}$  are the curvatures.

$$k_x = \frac{\partial^2 f(x, y)}{\partial x^2}, \quad k_y = \frac{\partial^2 f(x, y)}{\partial y^2}, \quad k_{xy} = k_{yx} = \frac{\partial^2 f(x, y)}{\partial x \partial y}. \quad (1-2)$$

The equations of equilibrium are

$$\frac{\partial N_x}{\partial x} + \frac{\partial N_{yx}}{\partial y} - k_x Q_x = 0, \quad (1-3)$$

$$\frac{\partial N_y}{\partial y} + \frac{\partial N_{xy}}{\partial x} - k_y Q_y = 0, \quad (1-4)$$

$$k_x N_x + 2k_{xy} N_{xy} + k_y N_y + \frac{\partial Q_x}{\partial x} + \frac{\partial Q_y}{\partial y} + p = 0, \quad (1-5)$$

$$Q_x = \frac{\partial M_x}{\partial x} + \frac{\partial M_{yx}}{\partial y}, \quad (1-6)$$

$$Q_y = \frac{\partial M_y}{\partial y} + \frac{\partial M_{xy}}{\partial x}, \quad (1-7)$$

where

$$M_{xy} = M_{yx}, \quad N_{xy} = N_{yx}. \quad (1-8)$$

As the veneers are symmetrically laminated, the coupling of "the membrane stress and the bending moment" does not occur. So that the strain-displacement relations of the neutral plane are

$$\epsilon_x = \frac{\partial u}{\partial x} - k_x w, \quad (1-9)$$

$$\epsilon_y = \frac{\partial v}{\partial y} - k_y w, \quad (1-10)$$

$$\gamma_{xy} = \frac{\partial u}{\partial y} + \frac{\partial v}{\partial x} - 2k_{xy} w. \quad (1-11)$$

And the strain (caused by bending)—deflection relations are

$$\epsilon_{xb} = -zw_{,xx}, \quad (1-12)$$

$$\epsilon_{yb} = -zw_{,yy}, \quad (1-13)$$

$$\gamma_{xy} = -2zw_{,xy} \quad (1-14)$$

$$\text{where} \quad w_{,xx} = \frac{\partial^2 w}{\partial x^2}, \quad w_{,yy} = \frac{\partial^2 w}{\partial y^2}, \quad w_{,xy} = \frac{\partial^2 w}{\partial x \partial y}. \quad (1-15)$$

As the veneer can be considered as an orthotropic material, the stress-strain relations in the  $n$ -th layer are

$$\begin{pmatrix} \sigma_{xn} \\ \sigma_{yn} \\ \tau_{xy_n} \end{pmatrix} = \begin{pmatrix} C_{11n} & C_{12n} & C_{16n} \\ C_{21n} & C_{22n} & C_{26n} \\ C_{61n} & C_{62n} & C_{66n} \end{pmatrix} \begin{pmatrix} \varepsilon_x \\ \varepsilon_y \\ \gamma_{xy} \end{pmatrix}, \quad (1-16)$$

$$\text{where} \quad C_{12n} = C_{21n}, \quad C_{16n} = C_{61n}, \quad C_{26n} = C_{62n}. \quad (1-17)$$

The membrane stress resultants and the bending moment resultants are obtained by the integration of (1-16) over each lamina and totalizing over all laminae. Thus :

$$\begin{aligned} N_x &= \sum_{n=1}^m \int_{h_{n-1}}^{h_n} \sigma_{xn} dz, & M_x &= \sum_{n=1}^m \int_{h_{n-1}}^{h_n} \sigma_{xn} z dz, \\ N_y &= \sum_{n=1}^m \int_{h_{n-1}}^{h_n} \sigma_{yn} dz, & M_y &= \sum_{n=1}^m \int_{h_{n-1}}^{h_n} \sigma_{yn} z dz, \\ N_{xy} &= \sum_{n=1}^m \int_{h_{n-1}}^{h_n} \tau_{xy_n} dz, & M_{xy} &= \sum_{n=1}^m \int_{h_{n-1}}^{h_n} \tau_{xy_n} z dz, \end{aligned} \quad (1-18) \sim (1-23)$$

where  $h_n$  denotes distance from the neutral plane to the lower face of  $n$ -th lamina (numbering from upper face lamina).

Using the following notations  $A_{ij}$ ,  $D_{ij}$  :

$$A_{ij} = \sum_{n=1}^m C_{ijn} (h_n - h_{n-1}) = \sum_{n=1}^m C_{ijn} t_n, \quad (1-24)$$

$$D_{ij} = \frac{1}{3} \sum_{n=1}^m C_{ijn} (h_n^3 - h_{n-1}^3) = \sum_{n=1}^m C_{ijn} I_n, \quad (1-25)$$

$$\text{where} \quad I_n = \frac{1}{3} (h_n^3 - h_{n-1}^3), \quad (1-26)$$

the stress and moment resultants are expressed as follows by substitution of (1-16) into (1-18)~(1-23) :

$$\begin{aligned} N_x &= \sum_{n=1}^m \int_{h_{n-1}}^{h_n} (C_{11n} \varepsilon_x + C_{12n} \varepsilon_y + C_{16n} \gamma_{xy}) dz \\ &= \varepsilon_x \sum_{n=1}^m C_{11n} (h_n - h_{n-1}) + \varepsilon_y \sum_{n=1}^m C_{12n} (h_n - h_{n-1}) + \gamma_{xy} \sum_{n=1}^m C_{16n} (h_n - h_{n-1}) \\ &= A_{11} \varepsilon_x + A_{12} \varepsilon_y + A_{16} \gamma_{xy}, \end{aligned} \quad (1-27)$$

$$\begin{pmatrix} N_x \\ N_y \\ N_{xy} \end{pmatrix} = \begin{pmatrix} A_{11} & A_{12} & A_{16} \\ A_{12} & A_{22} & A_{26} \\ A_{16} & A_{26} & A_{66} \end{pmatrix} \begin{pmatrix} \varepsilon_x \\ \varepsilon_y \\ \gamma_{xy} \end{pmatrix} \quad (1-28)$$

$$\begin{aligned}
 M_x &= \sum_{n=1}^m \int_{h_{n-1}}^{h_n} (C_{11n}\epsilon_{xb} + C_{12n}\epsilon_{yb} + C_{16n}\gamma_{xyb}) z dz \\
 &\quad \text{(substitute (1-12)~(1-15))} \\
 &= \sum_{n=1}^m \int_{h_{n-1}}^{h_n} -z^2 (C_{11n}w_{,xx} + C_{12n}w_{,yy} + 2C_{16n}w_{,xy}) dz \\
 &= - \sum_{n=1}^m \left[ \frac{1}{3} (h_n^3 - h_{n-1}^3) (C_{11n}w_{,xx} + C_{12n}w_{,yy} + 2C_{16n}w_{,xy}) \right] \\
 &= - (D_{11}w_{,xx} + D_{12}w_{,yy} + 2D_{16}w_{,xy}), \tag{1-29}
 \end{aligned}$$

$$\begin{pmatrix} M_x \\ M_y \\ M_{xy} \end{pmatrix} = - \begin{pmatrix} D_{11} & D_{12} & D_{16} \\ D_{12} & D_{22} & D_{26} \\ D_{16} & D_{26} & D_{66} \end{pmatrix} \begin{pmatrix} w_{,xx} \\ w_{,yy} \\ 2w_{,xy} \end{pmatrix} \tag{1-30}$$

Combining the all above equations (1-1)~(1-30) with the following stress function  $\phi$ , the fundamental equations can be derived in the more simply form.

$$N_x = \frac{\partial^2 \phi}{\partial y^2}, \quad N_y = \frac{\partial^2 \phi}{\partial x^2}, \quad N_{xy} = -\frac{\partial^2 \phi}{\partial x \partial y}. \tag{1-31}$$

This stress function satisfies the equations (1-3) and (1-4). Because the terms  $k_x Q_x$  and  $k_y Q_y$  can be neglected when the shells are shallow.

From the equations of equilibrium (1-5)~(1-8), the following differential equation is obtained :

$$\frac{\partial^2 M_x}{\partial x^2} + 2 \frac{\partial^2 M_{xy}}{\partial x \partial y} + \frac{\partial^2 M_y}{\partial y^2} + k_x N_x + 2k_{xy} N_{xy} + k_y N_y + p = 0 \tag{1-32}$$

The substitution of (1-30) and (1-31) in (1-32) yields the equation of equilibrium :

$$\begin{aligned}
 &D_{11} \frac{\partial^4 w}{\partial x^4} + 4D_{16} \frac{\partial^4 w}{\partial x^3 \partial y} + (2D_{12} + 4D_{66}) \frac{\partial^4 w}{\partial x^2 \partial y^2} + 4D_{26} \frac{\partial^4 w}{\partial x \partial y^3} \\
 &+ D_{22} \frac{\partial^4 w}{\partial y^4} - k_y \frac{\partial^2 \phi}{\partial x^2} + 2k_{xy} \frac{\partial^2 \phi}{\partial x \partial y} - k_x \frac{\partial^2 \phi}{\partial y^2} - p = 0 \tag{1-33}
 \end{aligned}$$

And the compatibility equation is derived from (1-9)~(1-11) :

$$\frac{\partial^2 \epsilon_x}{\partial y^2} + \frac{\partial^2 \epsilon_y}{\partial x^2} - \frac{\partial^2 \gamma_{xy}}{\partial x \partial y} + k_x \frac{\partial^2 w}{\partial y^2} - 2k_{xy} \frac{\partial^2 w}{\partial x \partial y} + k_y \frac{\partial^2 w}{\partial x^2} = 0 \tag{1-34}$$

Substituting eq. (1-28) and (1-31) into this equation, the compatibility equation is expressed by  $\phi$  and :

$$\begin{aligned}
 &B_{22} \frac{\partial^4 \phi}{\partial x^4} - 2B_{26} \frac{\partial^4 \phi}{\partial x^3 \partial y} + (2B_{12} + B_{66}) \frac{\partial^4 \phi}{\partial x^2 \partial y^2} - 2B_{16} \frac{\partial^4 \phi}{\partial x \partial y^3} + B_{22} \frac{\partial^4 \phi}{\partial y^4} \\
 &+ k_y \frac{\partial^2 w}{\partial x^2} - 2k_{xy} \frac{\partial^2 w}{\partial x \partial y} + k_x \frac{\partial^2 w}{\partial y^2} = 0, \tag{1-35}
 \end{aligned}$$

where  $[B_{ij}] = [A_{ij}]^{-1}$ . (1-36)

## 2. Relations between the Coefficients ( $B_{ij}$ , $D_{ij}$ ) and the Moduli of Elasticity

In this chapter, the following problems, about the relations between the coefficients ( $B_{ij}$ ,  $D_{ij}$ ) and the moduli of elasticity, are given the proof. Coefficients  $D_{ij}$  in the equilibrium equation (1-32) can be obtained by using the moduli of elasticity of "bending" ( $E_{xb}$ ,  $E_{yb}$ ,  $G_{xyb}$  and  $\mu_{xyb}$ ) of the plywood strips which have the same veneers and adhesives and the same construction of lamination as the plywood shells, whose lamination is symmetric with respect to the middle plane. And the coefficients  $B_{ij}$  in the compatibility equation (1-35) can be obtained by using the equations shown in (3-17), and the moduli of elasticity of "compression" (or tension) ( $E_{xc}$ ,  $E_{yc}$ ,  $G_{xyc}$  and  $\mu_{xyc}$ ) of the same plywood strips. When the axes of elastic symmetry (directions of the grain) do not coincide with the axes of coordinates (directions of the edges),  $B_{ij}$  and  $D_{ij}$  are obtained by the application of the equations of the coordinate transformation (3-10)~(3-13) as if the plywood strips were veneers which have the same elastic constants as those of the plywood strips ( $E_{xb}$ ,  $E_{xc}$ , ...).

It is better to get the coefficients  $B_{ij}$  and  $D_{ij}$  by the above-mentioned method which uses the moduli of elasticity of "the plywood" strips than by the calculation according to the equations (1-24), (1-25) and (1-36), which uses the moduli of elasticity of "the veneers". Because the former method gives the coefficients  $B_{ij}$  and  $D_{ij}$  which include the effect of the adhesion and the effect of the change of the specific gravity of the veneers by pressing.

Considering that the plywood shells and plywood strips are constituted by not only veneers but also "adhesive layers", the problems mentioned above can be given the proof as follows:

The elastic constant  $E_{xc}$  (nominal Young's modulus of the plywood strip which has the same construction of lamination as the plywood shells) is the ratio of  $N_x/t$  to  $\varepsilon_x$  when  $N_x \neq 0$  and  $N_y = N_{xy} = 0$ , *i. e.*

$$E_{xc} = \frac{N_x}{\varepsilon_x t} \quad \text{when } N_x \neq 0 \text{ and } N_y = N_{xy} = 0. \quad (2-1)$$

When the fiber directions (axes of elastic symmetry) coincide with the axes of coordinates, the equation of stress resultant (1-28) is expressed as follows;

$$\begin{pmatrix} N_x \\ N_y \\ N_{xy} \end{pmatrix} = \begin{pmatrix} A_{I I} & A_{I II} & 0 \\ A_{II I} & A_{II II} & 0 \\ 0 & 0 & A_{III} \end{pmatrix} \begin{pmatrix} \varepsilon_x \\ \varepsilon_y \\ \gamma_{xy} \end{pmatrix} \quad (2-2)$$

Substituting the stress conditions (2-1) *i. e.*  $N_x \neq 0$  and  $N_y = N_{xy} = 0$  in this equation,  $\varepsilon_x$ , under that stress condition, is expressed as follows;

$$\varepsilon_x = \frac{A_{II II}}{A_{I I} A_{II II} - A_{I II}^2} N_x \quad (2-3)$$

So the Young's modulus of compression (or tension)  $E_{Xc}$  can be expressed using only  $A_{IJ}$  and  $t$  by the substitution of eq. (2-3) in (2-1) :

$$E_{Xc} = \frac{A_{I I} A_{I I I} - A_{I I I}^2}{A_{I I I} t} \quad (2-4)$$

In the same way,  $E_{Yc}$ ,  $G_{XYc}$ ,  $\mu_{XYc}$  and  $\mu_{YXc}$  are also expressed using only  $A_{IJ}$  and  $t$  as follows :

$$E_{Yc} = \frac{A_{I I} A_{I I I} - A_{I I I}^2}{A_{I I I} t} \quad \left( E_{Yc} = \frac{N_Y}{\epsilon_Y t} \quad \text{when } N_Y \neq 0, N_X = N_{XY} = 0 \right), \quad (2-5)$$

$$G_{XYc} = \frac{A_{\text{III}}}{t} \quad \left( G_{XYc} = \frac{N_{XY}}{\gamma_{XY} t} \quad \text{when } N_{XY} \neq 0, N_X = N_Y = 0 \right), \quad (2-6)$$

$$\mu_{XYc} = \frac{A_{I I I}}{A_{I I I}} \quad \left( \mu_{XYc} = -\frac{\epsilon_Y}{\epsilon_X} \quad \text{when } N_X \neq 0, N_Y = N_{XY} = 0 \right), \quad (2-7)$$

$$\mu_{YXc} = \frac{A_{I I I}}{A_{I I I}} = \frac{A_{I I I}}{A_{I I I}} \quad \left( \mu_{YXc} = -\frac{\epsilon_X}{\epsilon_Y} \quad \text{when } N_Y \neq 0, N_X = N_{XY} = 0 \right). \quad (2-8)$$

Denoting  $C_{IJc}$  and  $C_{IJn}$  as follows :

$$C_{I I n} = \frac{E_{Xn}}{\lambda_n}, \quad C_{I I I n} = \frac{E_{Yn}}{\lambda_n}, \quad C_{I I I n} = \frac{\mu_{XYn} E_{Yn}}{\lambda_n}, \quad C_{\text{III} n} = G_{XYn},$$

$$\lambda_n = 1 - \mu_{XYn} \mu_{YXn}, \quad (2-9)$$

$$C_{I I c} = \frac{E_{Xc}}{\lambda_c}, \quad C_{I I I c} = \frac{E_{Yc}}{\lambda_c}, \quad C_{I I I c} = \frac{\mu_{XYc} E_{Yc}}{\lambda_c}, \quad C_{\text{III} c} = G_{XYc}$$

and  $\lambda_c = 1 - \mu_{XYc} \mu_{YXc}$  , (2-10)

$A_{IJ}$  are expressed in only  $t$  and  $C_{IJc}$  by substitution (2-5)~(2-8) in (2-9) :

$$\lambda_c = \frac{A_{I I} A_{I I I} - A_{I I I}^2}{A_{I I} A_{I I I}} \quad (2-11)$$

$$C_{I I c} = \frac{A_{I I}}{t}, \quad C_{I I I c} = \frac{A_{I I I}}{t}, \quad C_{I I I c} = \frac{A_{I I I}}{t}, \quad C_{\text{III} c} = \frac{A_{\text{III}}}{t}, \quad (2-12)$$

*i. e.*

$$A_{IJ} = C_{IJc} t. \quad (2-13)$$

Then,  $A_{IJ}$  can be obtained from  $E_{Xc}$ ,  $E_{Yc}$ ,  $G_{XYc}$  and  $\mu_{XYc}$  which are measured by "the tension (or compression)" of the strips made of the same construction of lamination as the plywood shallow shells. And it is now given the proof that the coefficients  $B_{ij}$  of the compatibility equation (1-35) can be obtained from the measured moduli of elasticity  $E_{Xc}$ ,  $E_{Yc}$ ,  $G_{XYc}$  and  $\mu_{XYc}$ . Because  $B_{ij}$  values are obtained by inverting the matrix  $A_{ij}$ ,  $A_{ij}$  values are obtained by the coordinate transformation of  $A_{IJ}$ , which is expressed in the next chapter,  $A_{IJ}$  values are obtained from  $C_{IJc}$  by using the equation (2-13), and  $C_{IJc}$  is obtained from the measured value  $E_{Xc}$ ,  $E_{Yc}$ ,  $G_{XYc}$  and  $\mu_{XYc}$  :

$$(E_{Xc}, \dots) \longrightarrow C_{IJc} \longrightarrow A_{IJ} \longrightarrow A_{ij} \longrightarrow B_{ij} . \quad (2-14)$$



In the same way, it is also given the proof that the coefficients  $D_{ij}$  of the equilibrium equation (1-33) are obtained from  $E_{xb}$ ,  $E_{yb}$ ,  $G_{xyb}$  and  $\mu_{xyb}$  which are measured by "the bending" of the same plywood strips :

$$(E_{xb}, \dots) \longrightarrow C_{IJb} \longrightarrow D_{IJ} \longrightarrow D_{ij} . \quad (2-15)$$

In this case it is necessary only to change  $t \rightarrow I$ ,  $\varepsilon_x, \varepsilon_y, \gamma_{xy} \rightarrow w_{,xx}, w_{,yy}, 2w_{,xy}$ ,  $N \rightarrow M$ , and subscript  $c \rightarrow$  subscript  $b$  and use eq. (1-30) instead of eq. (1-28). For example, instead of eq. (2-1), following equation is used ;

$$E_{xb} = \frac{M_x}{w_{,xx}I} \text{ when } M_x \neq 0, M_y = M_{xy} = 0, \quad (2-16)$$

where  $w_{,xx}$  (see eq. (1-15)) is equal to curvature ( $1/\rho_x$ ) given by the bending of the plywood strips.

### 3. The Coordinate Transformation of the Elastic Constants

To complete the proof of last chapter, it is necessary to give the equations of the coordinate transformation<sup>7,8)</sup> for the layered plates (or the plywoods), whose laminae are orthotropic and are laminated parallel or perpendicular to the adjacent ones.

The equations of the transformation for the not laminated orthotropic plates (or the veneers) can be expressed as follows :

$$C_{11n} = C_{IIn} \cos^4 \theta + C_{IIIn} \sin^4 \theta + 2(C_{IIn} + 2C_{VVn}) \cos^2 \theta \sin^2 \theta, \quad (3-1)$$

$$C_{12n} = (C_{IIn} + C_{IIIn} - 4C_{VVn}) \cos^2 \theta \sin^2 \theta + C_{IIn} (\cos^4 \theta + \sin^4 \theta), \quad (3-2)$$

$$C_{16n} = (C_{IIn} \cos^2 \theta - C_{IIIn} \sin^2 \theta) \cos \theta \sin \theta - (C_{IIn} + 2C_{VVn}) \times (\cos^3 \theta \sin \theta - \cos \theta \sin^3 \theta), \quad (3-3)$$

$$C_{22n} = C_{IIn} \sin^4 \theta + C_{IIIn} \cos^4 \theta + 2(C_{IIn} + 2C_{VVn}) \cos^2 \theta \sin^2 \theta, \quad (3-4)$$

$$C_{26n} = (C_{IIn} \sin^2 \theta - C_{IIIn} \cos^2 \theta) \cos \theta \sin \theta + (C_{IIn} + 2C_{VVn}) \times (\cos^3 \theta \sin \theta - \cos \theta \sin^3 \theta), \quad (3-5)$$

$$C_{66n} = (C_{IIn} + C_{IIIn} - 2C_{IIn}) \cos^2 \theta \sin^2 \theta + C_{VVn} (\cos^2 \theta - \sin^2 \theta)^2, \quad (3-6)$$

where,  $C_{ijn}$  are elastic constants at coordinate direction (see eq. (1-16)), and  $C_{IJn}$  are elastic constants parallel to the axes of the elastic symmetry (parallel or perpendicular to the fiber direction), which are inclined  $\theta$  rad. to the coordinate axes. Substituting eq. (3-1) in eq. (1-24), the following equation is obtained :

$$A_{11} = \sum_{n=1}^m [C_{IIn} t_n \cos^4 \theta + C_{IIIn} t_n \sin^4 \theta + 2(C_{IIn} + 2C_{VVn}) t_n \cos^2 \theta \sin^2 \theta]. \quad (3-7)$$

As  $\theta$  is same in all laminae when the lamination is parallel or perpendicular as expressed above, this equation can be rewritten as follows :

$$A_{11} = \cos^4\theta \sum_{n=1}^m C_{111n}t_n + \sin^4\theta \sum_{n=1}^m C_{112n}t_n + 2\cos^2\theta\sin^2\theta \left( \sum_{n=1}^m C_{113n} + 2 \sum_{n=1}^m C_{114n} \right). \quad (3-8)$$

And as  $A_{IJ}$  can be written from eq. (1-24) as follows :

$$A_{IJ} = \sum_{n=1}^m C_{IJn}t_n, \quad (3-9)$$

the following relation is obtained :

$$A_{11} = A_{11} \cos^4\theta + A_{11} \sin^4\theta + 2(A_{11} + 2A_{11})\cos^2\theta\sin^2\theta. \quad (3-10)$$

In the same manner,  $A_{12}$ ,  $A_{16}$ ,  $A_{22}$ ,  $A_{26}$  and  $A_{66}$  are expressed in the same form, that is,  $C$  is replaced by  $A$ , subscripts  $ijn$  and  $IJn$  by  $ij$  and  $IJ$ , respectively, in eqs. (3-1)~(3-6). (3-11)

So the transformation equations of the elastic constants of the orthotropic layered plates, *i. e.*  $A_{IJ} \rightarrow A_{ij}$  are obtained.

And the transformation equations of the elastic constants for bending, *i. e.*  $D_{IJ} \rightarrow D_{ij}$ , are also obtained in the same manner, for example ;

$$D_{11} = D_{11} \cos^4\theta + D_{11} \sin^4\theta + 2(D_{11} + 2D_{11})\cos^2\theta\sin^2\theta. \quad (3-12)$$

$D_{12}$ ,  $D_{16}$ ,  $D_{22}$ ,  $D_{26}$  and  $D_{66}$  are also expressed by the replacement,  $C \rightarrow D$ , subscripts  $ijn \rightarrow ij$  and  $IJn \rightarrow IJ$  in eqs. (3-1)~(3-6). (3-13)

Expanding the range of the application of eq. (2-12),  $C_{ijc}$  is denoted as follows :

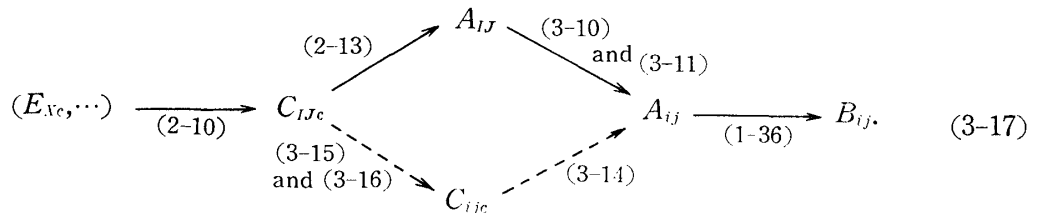
$$C_{ijc} = \frac{A_{ij}}{t}. \quad (3-14)$$

Substituting these relations (2-12) and (3-14) in the transformation equation (3-10) and (3-11), the following relation is obtained :

$$C_{11c} = C_{11c} \cos^4\theta + C_{11c} \sin^4\theta + 2(C_{11c} + 2C_{11c})\cos^2\theta\sin^2\theta, \quad (3-15)$$

and the same relations as eqs. (3-2)~(3-6), whose subscript  $n$  is changed to subscript  $c$ . (3-16)

So the route.....→shown below can also be given the proof.



And the following relation for the bending elastic constants are also given the proof :

$$\begin{array}{c}
 \begin{array}{ccc}
 & & D_{IJ} \\
 & \nearrow^{(2-13)*} & \\
 (E_{Xb}, \dots) & \xrightarrow{(2-10)*} & C_{IJb} \\
 & \searrow_{(3-15)*} & \\
 & & C_{ijb} \\
 & & \nearrow_{(3-16)*} \\
 & & D_{ij} \\
 & \nwarrow_{(3-14)*} & \\
 & & D_{IJ}
 \end{array}
 \end{array}
 \begin{array}{l}
 \\
 \\
 \\
 \text{and } (3-11)* \\
 \\
 \\
 \\
 \end{array}
 \quad (3-18)$$

\* change the notations of the equations to the bending type according to the manners expressed between (2-15) and (2-16).

Then, it is now proved that the coefficients of the fundamental equations of the layered orthotropic shells *i. e.*  $B_{ij}$  and  $D_{ij}$  can be calculated from the measured moduli of elasticity *i. e.*  $(E_{Xc}, E_{Yc}, G_{XYc}, \mu_{XYc})$  and  $(E_{Xb}, E_{Yb}, G_{XYb}, \mu_{XYb})$ , respectively as shown in (3-17) and (3-18). And this means that the coefficients can be calculated as if the shells were the not layered orthotropic shells with the nominal moduli of elasticity,  $E_{Xb}, E_{Yb}, \dots$  for the bending moments and  $E_{Xc}, E_{Yc}, \dots$  for the membrane stresses.

### Procedure of the Numerical Analysis by means of the Finite Difference Method

#### 1. The Finite Difference Equations of the Fundamental Equations

As it is very difficult to get the mathematically exact solution of the fundamental simultaneous equations (1-33) and (1-35), the finite difference method is applied to solve them approximately. The fundamental equations are replaced by the corresponding finite difference equations shown in Figs. 2 and 3 in the same

$$\begin{array}{ccc}
 \begin{array}{|c|c|c|} \hline -E_8 & E_6 & E_8 \\ \hline -E_9 & E_4 & E_2 & E_5 & E_9 \\ \hline E_7 & E_3 & E_1 & E_3 & E_7 \\ \hline E_9 & E_5 & E_2 & E_4 & -E_9 \\ \hline E_8 & E_6 & -E_8 \\ \hline \end{array} & + & \begin{array}{|c|c|c|} \hline -D_4 & D_2 & D_4 \\ \hline D_3 & D_1 & D_3 \\ \hline D_4 & D_2 & -D_4 \\ \hline \end{array} = p_k \cdot d_x^4, \\
 W & & \phi
 \end{array}$$

where,  $E_1 = 6D_{11} + (8D_{12} + 16D_{66})\lambda^{-2} + 6D_{22}\lambda^{-4}$   
 $E_2 = -(16D_{12} + 32D_{66})\lambda^{-2} - 4D_{22}\lambda^{-4}$   
 $E_3 = -4D_{11} - (4D_{12} + 8D_{66})\lambda^{-2}$   
 $E_4 = 2D_{16}\lambda^{-1} + (2D_{12} + 4D_{66})\lambda^{-2} + 2D_{26}\lambda^{-3}$   
 $E_5 = -2D_{16}\lambda^{-1} + (2D_{12} + 4D_{66})\lambda^{-2} - 2D_{26}\lambda^{-3}$   
 $E_6 = D_{22}\lambda^{-4}, E_7 = D_{11}, E_8 = D_{26}\lambda^{-3}, E_9 = D_{16}\lambda^{-1},$   
 $D_1 = 2k_x\lambda^{-2} + 2k_y, D_2 = -k_x\lambda^{-2}, D_3 = -k_y,$   
 $D_4 = \frac{1}{2}k_{xy}\lambda^{-1}, \lambda = \frac{dy}{dx}.$

Fig. 2. The finite difference equation of the equilibrium equation (1-33) at the nodal point k.

$$\begin{array}{|c|c|c|} \hline & -C_8 & C_6 & C_8 \\ \hline -C_9 & C_4 & C_2 & C_5 & C_9 \\ \hline C_7 & C_3 & C_1 & C_3 & C_7 \\ \hline C_9 & C_5 & C_2 & C_4 & -C_9 \\ \hline & C_8 & C_6 & -C_8 \\ \hline \end{array} \phi + \begin{array}{|c|c|c|} \hline D_4 & -D_2 & -D_4 \\ \hline -D_3 & -D_1 & -D_3 \\ \hline -D_4 & -D_2 & D_4 \\ \hline \end{array} W = 0,$$

where,  $C_1=6B_{22}+(8B_{12}+4B_{66})\lambda^{-2}+6B_{11}\lambda^{-4}$   
 $C_2=-(4B_{12}+2B_{66})\lambda^{-2}-4B_{11}\lambda^{-4}$   
 $C_3=-4B_{22}-(4B_{12}+2B_{66})\lambda^{-2}$   
 $C_4=-B_{26}\lambda^{-1}+(2B_{12}+B_{66})\lambda^{-2}-B_{16}\lambda^{-3}$   
 $C_5=B_{26}\lambda^{-1}+(2B_{12}+B_{66})\lambda^{-2}+B_{16}\lambda^{-3}$   
 $C_6=B_{11}\lambda^{-4}, C_7=B_{22},$   
 $C_8=-\frac{1}{2}B_{16}\lambda^{-3}, C_9=-\frac{1}{2}B_{26}\lambda^{-1}.$

Fig. 3. The finite difference equation of the compatibility equation (1-35) at the nodal point k.

manner as written in the previous report "Numerical Analysis of Orthotropic Plates"<sup>9)</sup>.

### 2. The Finite Difference Equations of the Boundary Conditions

In this paper, the application of the finite difference methods to the problems of the layered orthotropic shallow shells with "four edges simply supported by means of rollers" is discussed. This roller-support boundary condition can be expressed as follows:

on the edges parallel to the y axis, i. e.  $x = \pm a/2,$   
 $w = M_x = N_x = \epsilon_y \text{ (or } v) = 0,$  (4-1)

on the edges parallel to the x axis, i. e.  $y = \pm b/2,$   
 $w = M_y = N_y = \epsilon_x \text{ (or } u) = 0.$  (4-2)

These boundary conditions are also expressed by using only  $w$  and  $\phi$ . The bending moments and the membrane stresses are expressed by using the equations (1-30) and (1-31), respectively. And the membrane strains are expressed as follows from eqs. (1-28), (1-31) and (1-36):

$$\begin{pmatrix} \epsilon_x \\ \epsilon_y \\ \gamma_{xy} \end{pmatrix} = \begin{pmatrix} B_{11} & B_{12} & B_{16} \\ B_{12} & B_{22} & B_{26} \\ B_{16} & B_{26} & B_{66} \end{pmatrix} \begin{pmatrix} \frac{\partial^2 \phi}{\partial y^2} \\ \frac{\partial^2 \phi}{\gamma x^2} \\ -\frac{\partial^2 \phi}{\partial x \partial y} \end{pmatrix}. \tag{4-3}$$

These equations can also be replaced by the corresponding finite difference equations as shown in Fig. 4.

$$M_x|_k = \frac{1}{2d_x^2} \times \begin{matrix} R_{14} & R_{12} & -R_{14} \\ R_{13} & R_{11} & R_{13} \\ -R_{14} & R_{12} & R_{14} \end{matrix} \phi$$

$$N_x|_k = \frac{1}{d_x^2 \lambda^2} \times \begin{matrix} 1 \\ -2 \\ 1 \end{matrix} \phi$$

$$\epsilon_y|_k = \frac{1}{d_x^2} \times \begin{matrix} P_{24} & P_{22} & -P_{24} \\ P_{23} & P_{21} & P_{23} \\ -P_{24} & P_{22} & P_{24} \end{matrix} \phi$$

$R_{11} = 4D_{11} + 4D_{12}\lambda^{-2}$   
 $R_{12} = -2D_{12}\lambda^{-2}$   
 $R_{13} = -2D_{11}$   
 $R_{14} = D_{16}\lambda^{-1}$   
 $\lambda = d_y/d_x.$

$P_{21} = -2B_{12}\lambda^{-2} - 2B_{22}$   
 $P_{22} = B_{12}\lambda^{-2}$   
 $P_{23} = B_{22}$   
 $P_{24} = \frac{1}{4}B_{26}\lambda^{-1}$

Fig. 4. The finite difference equations of the bending moment  $M_x$ , the membrane stress  $N_x$  and the membrane strain  $\epsilon_y$  at the nodal point k.

### 3. Computation Procedure

In order to solve the simultaneous linear equations consist of the above finite difference equations of "the fundamental equations and the boundary conditions",

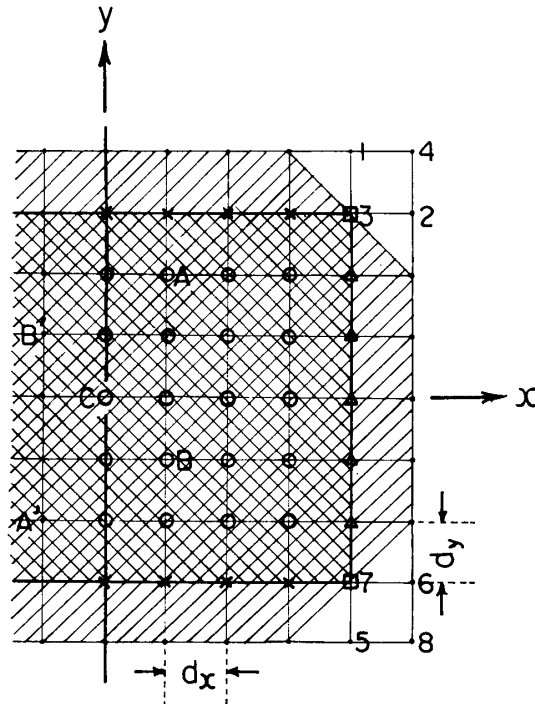


Fig. 5. An example of the meshes of the finite difference method.

the number of the equations must be equal to that of the unknowns. Taking advantage of symmetry with respect to the central point C, for example,  $w_A = w_{A'}$ ,  $w_B = w_{B'}$ ..., only the half of the shell is considered as shown in Fig. 5.

1) The finite difference equations of the equilibrium equation and the compatibility equation hold at each nodal point of symbol  $\circ$  in Fig. 5.

2) The finite difference equations of the boundary conditions (4-1) and (4-2) hold at each nodal point of  $\triangle$  and  $\times$ , respectively.

3) On the corner points  $\square$ ,  $w_3$  and  $w_7$  are equal to zero.

The number of the finite difference equations is smaller than that of the unknowns by four and six about  $w$  and  $\phi$ , respectively. To equalize these, the following relations are used:

$$w_1 = w_2 = w_5 = w_6 = 0, \tag{4-4}$$

$$\phi_1 = \phi_2 = \phi_3 = \phi_5 = \phi_6 = \phi_7 = 0. \tag{4-5}$$

The relations (4-5) are equivalent to “ $N_x = N_y = 0$  at the corners”. And the relations (4-4) means that the deflections of the imaginary nodal points on the extended lines of the edges are equal to zero. These are equivalent to “ $M_x = M_y = 0$  at the corners” when the axes of elastic symmetry coincide with the axes of coordinates, but are not equivalent when those do not coincide.

As the imaginary nodal points 4 and 8 in Fig. 5 are not used, the values of  $M_x$ ,  $M_y$ ,  $M_{xy}$  and  $N_{xy}$  at the corners are calculated by means of the extrapolation.

Thus, the simultaneous linear equations *i. e.* the finite difference equations are obtained in the following form:

$$\begin{pmatrix} \text{equilibrium equations} \\ \text{compatibility equations} \\ \text{boundary conditions} \end{pmatrix} \begin{pmatrix} w_k \\ \dots \\ \phi_k \end{pmatrix} = \begin{pmatrix} p_k \\ 0 \\ 0 \end{pmatrix}. \tag{4-6}$$

As the matrices of these simultaneous equations are large and complicated (for example,  $86 \times 86$  for  $8 \times 8$  meshes and  $128 \times 128$  for  $10 \times 10$  meshes), the authors designed the computer programs not only to solve the linear equations but also to make the matrices. So the accuracy of the approximation is easily examined by changing the input data card for the mesh sizes. Thus, the distributions of the deflection  $w$  and the stress function  $\phi$  are obtained by the computation, and then those of the bending moments and the membrane stresses are also calculated by using the equations shown in Fig. 4.

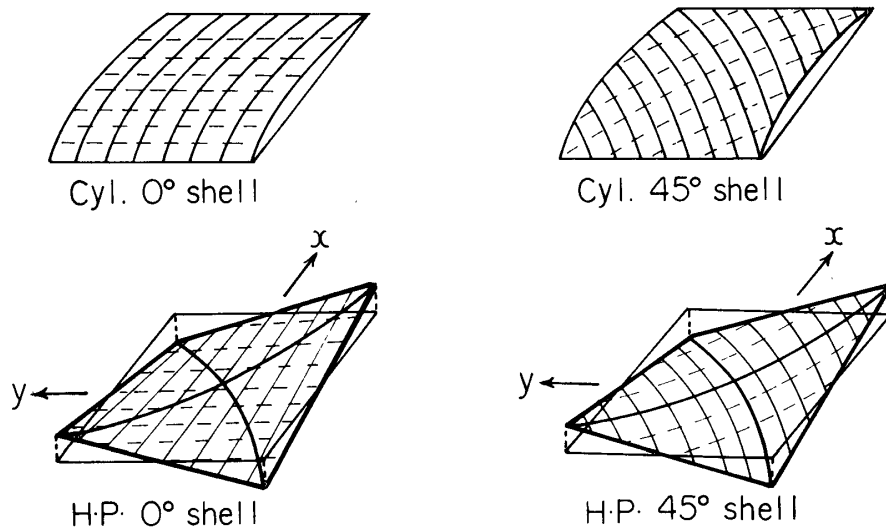


Fig. 6. Figures of the orthotropic plywood cylindrical shells and the H. P. shells, whose face grain (principal elastic axis) is parallel and/or inclined at  $45^\circ$  to the edges.

## Results and Discussions

### 1. Accuracy of the Solutions by the Finite Difference Method

As the finite difference method is one of the techniques to get approximate solution, it is necessary to examine the accuracy of the solution. The influence of the mesh sizes is shown in Figs. 7, 8 and 9. These figures show that the finite difference method mentioned above gives good approximate solutions to the problems of the roller-supported plywood shallow shells. The finer the mesh becomes, the more accurate solution can be obtained. But the capacity of the memory and the computation time give the limitation to the mesh sizes. So it is effective to apply the extrapolation method (see authors report<sup>9)</sup> p 23 eq. 16-2), when the more accurate solutions are needed.

As is evident from the figures, the results with the  $8 \times 8$  grid give the sufficiently accurate solutions to make clear the mechanical characteristics of the orthotropic plywood shallow shells. So the results computed with the  $8 \times 8$  meshes are used in the following discussions.

### 2. Effect of the Curvature

#### *Deflection*

The effect of the curvature on the deflection of the orthotropic plywood cylindrical shallow shells is shown in Fig. 10, and that of the hyperbolic paraboloidal (H. P.) shells is in Fig. 11. And the effect of the rise on the central deflection<sup>10)</sup> is shown in Fig. 12. As is evident from the figures, the effect of the curvature on

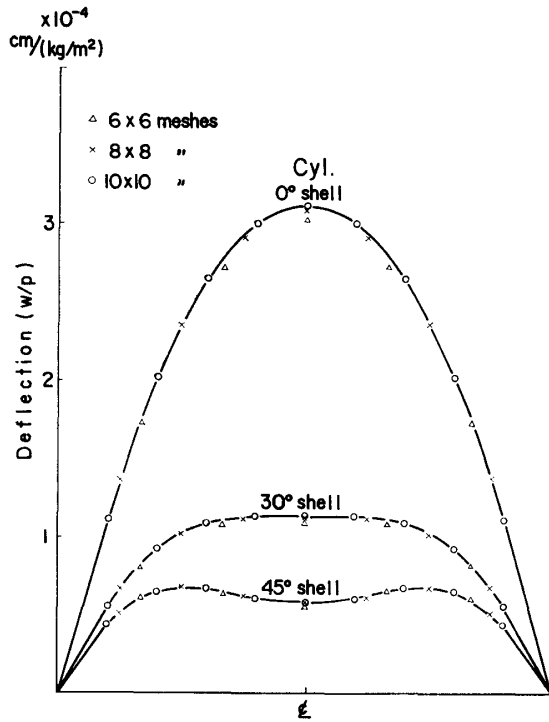


Fig. 7. Influence of mesh sizes on the deflection along the central curved line of the orthotropic cylindrical shells\* ( $k_x=0.01$  or rise/span=0.075) under uniform pressure.  $0^\circ$ ,  $30^\circ$  and  $45^\circ$  denote the shells whose principal elastic axes are inclined to the edges at  $0^\circ$ ,  $30^\circ$  and  $45^\circ$ , respectively.

\* The dimension of the shells is  $60\text{ cm} \times 60\text{ cm} \times 0.9\text{ cm}$ . The moduli of elasticity are equal to those of  $C$  in Table 2.

\*\* When the case \*\*\*\* in Table 2, the unit of the scale is  $\times 10^{-3}\text{ cm}/(\text{kg}/\text{m}^2)$ .

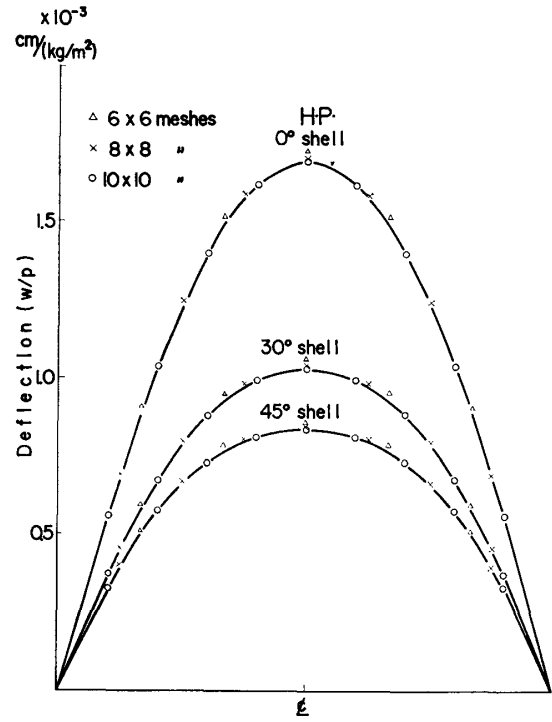
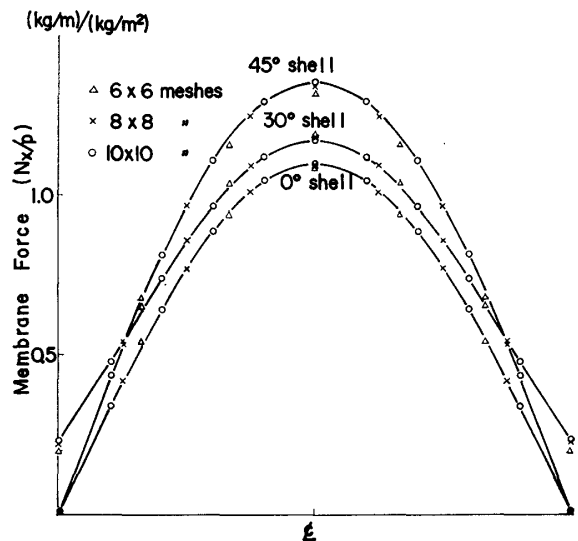


Fig. 8. Influence of mesh sizes on the deflection (along the central line parallel to  $x$  axis) of the orthotropic H. P. shells ( $k_{xy}=0.005$ ). See \* in Fig. 7.

\* When the case \*\*\*\* in Table 2, the unit of the scale is  $\times 10^{-2}\text{ cm}/(\text{kg}/\text{cm}^2)$ .

Fig. 9. Influence of mesh sizes on the membrane force  $N_x$  along the central curved line of the orthotropic cylindrical square shells (the same shells as shown in Fig. 7).

\* When the case \*\*\*\* in Table 2, the unit of the scale is  $\times 10\text{ (kg/m)}/(\text{kg}/\text{m}^2)$ .





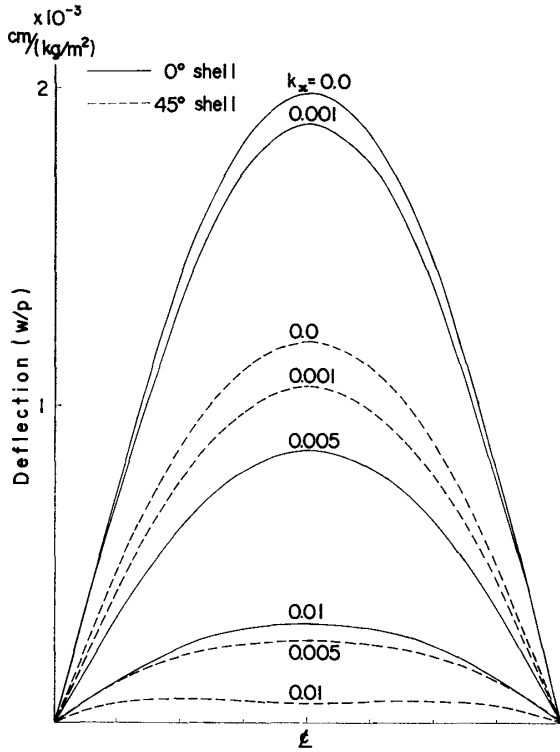


Fig. 10. Effect of the curvature on the deflection (along the central line parallel to  $x$  axis) of the orthotropic cylindrical shells under uniform pressure. See \* in Fig. 7 and 8.

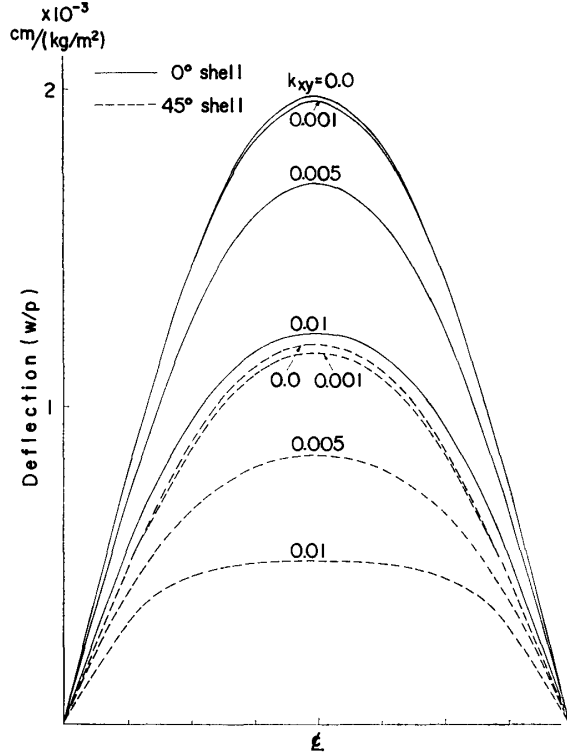


Fig. 11. Effect of the curvature on the deflection (along the central line parallel to  $x$  axis) of the H. P. shells under uniform pressure. See \* in Fig. 7 and 8.

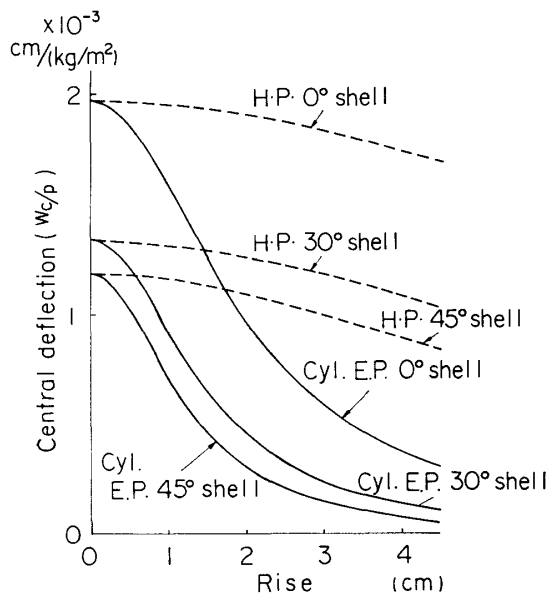


Fig. 12. Effect of the rise (or the curvature) on the central deflection of the shells (cylindrical, H. P. and E. P.) under uniform pressure. See \* in Fig. 7 and 8.

Cyl.— $k_x \neq 0, k_y = k_{xy} = 0$ , “ $k_x = 0.01$ ” is equal to “rise = 4.5 cm”

H. P.— $k_x = k_y = 0, k_{xy} \neq 0$ , “ $k_{xy} = 0.005$ ” is equal to “rise = 4.5 cm”

E. P.— $k_x = k_y \neq 0, k_{xy} = 0$ , “ $k_x = k_y = 0.005$ ” is equal to “rise = 4.5 cm”

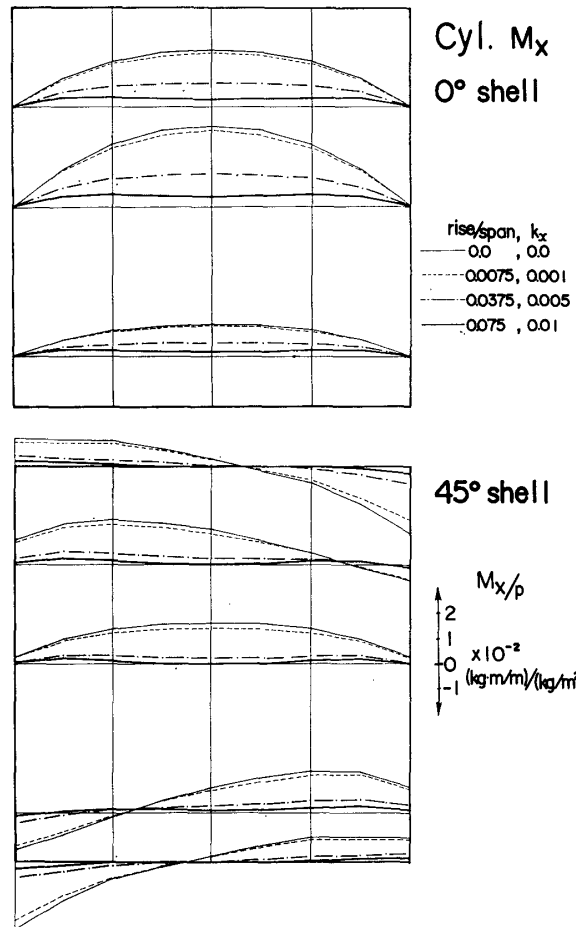


Fig. 13. Effect of the curvature on the bending moment of the orthotropic cylindrical shells under uniform pressure. See \* in Fig. 7. When the case \*\*\*\* in Table 2, the unit of the scale is  $\times (\text{kg}\cdot\text{m}/\text{m})/(\text{kg}/\text{m}^2)$ .

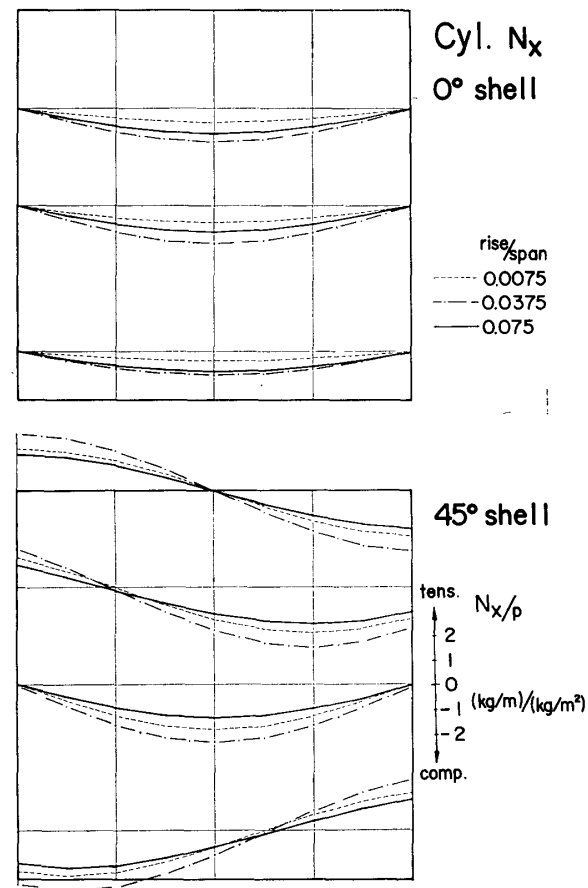


Fig. 14. Effect of the curvature on the membrane force of the orthotropic cylindrical shells under uniform pressure. See \* in Fig. 7 and 9.

rise on the deflection of the cylindrical (Cyl.) shells with four edges roller-supported is much larger than that on the deflection of the H. P. shells. And the effect of rise on the deflection of the cylindrical shells is almost the same as that of the elliptic paraboloidal (E. P.) shells.<sup>10)</sup> As is shown in Fig. 10, the central part of the deflection curve is depressed when the rise increases.

#### *Bending Moment and Membrane Stress*

The effect of the curvature on the bending moment and the membrane stress of the cylindrical shell is shown in Figs. 13 and 14. The bending moment parallel to the face grain decreases as the curvature increases. The membrane stress is equal to zero when the curvature is equal to zero (*i. e.* the plates), and it increases as the curvature increases. But it begins to decrease when the curvature becomes larger than a certain amount, as shown in Fig. 14. This phenomenon can be explained by the increase of the stress component against the external force.

The average face-strain caused by the bending moments is almost the same as that caused by the membrane stresses when the curvature  $k_x$  is about 0.01.

### 3. Influence of "the Direction of the Axes of Elastic Symmetry" and "the Moduli of Elasticity".

#### *Direction of the Axes of the Elastic Symmetry*

The central deflection of the square plates and shells under uniform pressure is shown in Table 2.

The deflection of the square shells becomes smallest when the direction of the axes of elastic symmetry inclines at  $45^\circ$  to that of the edges, except the case of A (parallel laminated shells). This is one of the interesting characteristics of the orthotropic plates and shells.

The deflection of  $0^\circ$  shell (the elastic principal axis is parallel to the edges or to the  $x$  axis) is almost the same as that of  $90^\circ$  shell except the case of A-Cyl. in Table 2.

Examining Table 2 with consideration that "the bending elastic constants of cases B and C and/or D and E" and "the compression (or tension) elastic constants of cases B and D and/or C and E" are equal to each other, it becomes clear that the effect of the membrane stress to the deflection becomes larger than that of the bending moment as the rise increases.

Except the extreme case of  $E_x \gg E_y$  as case A in Table 2, the deflection curves of the orthotropic plates and shells are similar to each other (in the cases of B, C, D and E). The deflection of the "isotropic" plates and shells, whose elastic constants are equivalent to the orthotropic plates and shells, is shown in Fig. 10.

Table 2. Influence of "the moduli of elasticity", "the curvature" and "the direction of the axes of elastic symmetry" to the central deflection under uniform pressure.\*

Moduli of elasticity of the plates and shells $\times 10^3 \text{ kg/cm}^{2***}$		$\theta$	Central deflection ( $w_c/p$ ) $\times 10^{-3} \text{ cm}/(\text{kg/m}^2)****$					
			Plate $k_x=k_y=$ $k_{xy}=0$	Cyl. $k_x=0.001$ $k_y=k_{xy}=0$	Cyl. $k_x=0.005$ $k_y=k_{xy}=0$	Cyl. $k_x=0.01$ $k_y=k_{xy}=0$	E. P. $k_x=k_y=$ $0.005$ $k_{xy}=0$	H.P $k_x=k_y=0$ $k_{xy}=0.005$
A	$E_{Xb}=145$ $E_{Xc}=145$	$0^\circ$	1.859	1.815	1.120	0.498	0.477	1.692
	$E_{Yb}=5$ $E_{Yc}=5$	$30^\circ$	1.813	1.787	1.337	0.767	0.747	1.620
	$G_{XYb}=5$ $G_{XYc}=5$	$45^\circ$	1.734	1.710	1.277	0.718	0.709	1.539
	$\mu_{XYb}=0.55$ $\mu_{XYc}=0.55$	$90^\circ$	1.859	1.804	1.029	0.393**	0.477	1.692
B	$E_{Xb}=100$ $E_{Xc}=100$	$0^\circ$	1.981	1.884	0.864	0.313	0.308	1.707
	$E_{Yb}=50$ $E_{Yc}=50$	$30^\circ$	1.342	1.237	0.419	0.125	0.121	1.054
	$G_{XYb}=5$ $G_{XYc}=5$	$45^\circ$	1.191	1.064	0.283	0.069	0.068	0.865
	$\mu_{XYb}=0.055$ $\mu_{XYc}=0.055$	$90^\circ$	1.981	1.884	0.858	0.302	0.308	1.707
C	$E_{Xb}=100$ $E_{Xc}=75$	$0^\circ$	1.981	1.883	0.856	0.309	0.304	1.703
	$E_{Yb}=50$ $E_{Yc}=75$	$30^\circ$	1.342	1.227	0.390	0.112	0.109	1.039
	$G_{XYb}=5$ $G_{XYc}=5$	$45^\circ$	1.191	1.048	0.250	0.057	0.056	0.842
	$\mu_{XYb}=0.055$ $\mu_{XYc}=0.037$	$90^\circ$	1.981	1.883	0.851	0.299	0.304	1.703
D	$E_{Xb}=75$ $E_{Xc}=100$	$0^\circ$	1.984	1.888	0.864	0.310	0.309	1.711
	$E_{Yb}=75$ $E_{Yc}=50$	$30^\circ$	1.303	1.204	0.415	0.123	0.121	1.041
	$G_{XYb}=5$ $G_{XYc}=5$	$45^\circ$	1.142	1.026	0.281	0.069	0.068	0.851
	$\mu_{XYb}=0.037$ $\mu_{XYc}=0.055$	$90^\circ$	1.984	1.888	0.863	0.309	0.309	1.711
E	$E_{Xb}=75$ $E_{Xc}=75$	$0^\circ \& 90^\circ$	1.984	1.887	0.857	0.306	0.305	1.708
	$E_{Yb}=75$ $E_{Yc}=75$	$30^\circ$	1.303	1.194	0.385	0.110	0.109	1.022
	$G_{XYb}=5$ $G_{XYc}=5$	$45^\circ$	1.142	1.009	0.248	0.057	0.056	0.822
F	$E_b=E_c=54.3$	—	1.441	1.289	0.352	0.095	0.096	1.062
	$E_b=E_c=20.8$							
	$\mu_b=\mu_c=0.309$							

\* The dimension of the plates and shells is 60cm×60cm×0.9cm (thickness).

\*\* In this shell the deflection becomes maximum (0.441) near the mid point between the not curved edge and the center of the shell.

\*\*\* except for  $\mu$

\*\*\*\* When the sizes of the plates and the shells are 6m×6m×9cm and the curvatures are 1/10 of this table *i. e.* the same rise/span ratio, the unit is  $\times 10^{-2} \text{ cm}/(\text{kg/m}^2)$ .

Table 2. These isotropic elastic constants are calculated with consideration that "the lamination and the adhesion of the infinitesimally thin veneers in every direction" make isotropic plates and shells. The values of the deflection of these isotropic plates and shells are between those of  $0^\circ$  and those of  $45^\circ$  of the orthotropic plates and shells (B, C, D and E in Table 2) except the case A.

Table 3. Rectangular plates and shells.\*

Curvature	$\theta$	Central deflection ( $w_c/p$ ) $\times 10^{-3}$ cm/(kg/m <sup>2</sup> )		
		square 1 : 1 (60cm $\times$ 60cm)**	rectangular 1 : 1.5 (60cm $\times$ 90cm)**	rectangular 1 : 2 (60cm $\times$ 120cm)**
Plate $k_x = k_y = k_{xy} = 0$	0°	1.981	2.818	3.012
	30°	1.342	2.516	3.345
	45°	1.191	2.423	3.531
	90°	1.981	4.295	5.522
Cyl. $k_x = 0.005$ $k_y = k_{xy} = 0$	0°	0.856	1.569	2.112
	30°	0.390	1.028	1.995
	45°	0.250	0.858	2.028
	90°	0.851	1.942	3.031
Cyl. $k_x = 0.01$ $k_y = k_{xy} = 0$	0°	0.309	0.669	1.089
	30°	0.112	0.363	0.890
	45°	0.057	0.278	0.873
	90°	0.299	0.720	1.278

\* the moduli of elasticity are the same as those of type C shown in Table 2.

\*\* See \*\*\*\* in Table 2.

*Rectangular Plates and Shells*

The central deflection of the rectangular cylindrical shells under uniform pressure is shown in Table 3. When the ratio of the side lengths is 1 : 2, the minimum central deflection is obtained at smaller angle than 45°.

**4. Distributions of the Deflection, the Bending Moments and the Membrane Forces under Uniform Pressure**

*Deflection*

Distributions of the deflection, the bending moments and the membrane forces of the “cylindrical” shells with the moduli of elasticity of type C (Table 2) “under uniform pressure” are shown in Figs. 15~21.

The deflection distributions of the cylindrical shells ( $k_x = 0.01$ , rise/span = 0.075) are shown in Fig. 15. The deflection curves of the 45° shell (face grain is inclined at 45°) and that of the isotropic shell (F in Table 2) are flat except near the edges, and those deflections are much smaller than that of the 0° shell.

*Bending Moments*

The distributions of the bending moment parallel to the elastic principal axis of the orthotropic shells ( $M_x$ ) are shown in Fig. 16 with the distribution of the maximum bending moment of the equivalent isotropic shell ( $M_{max}$ ). The bending moment of the 45° shell and that of the isotropic shell are smaller than that of

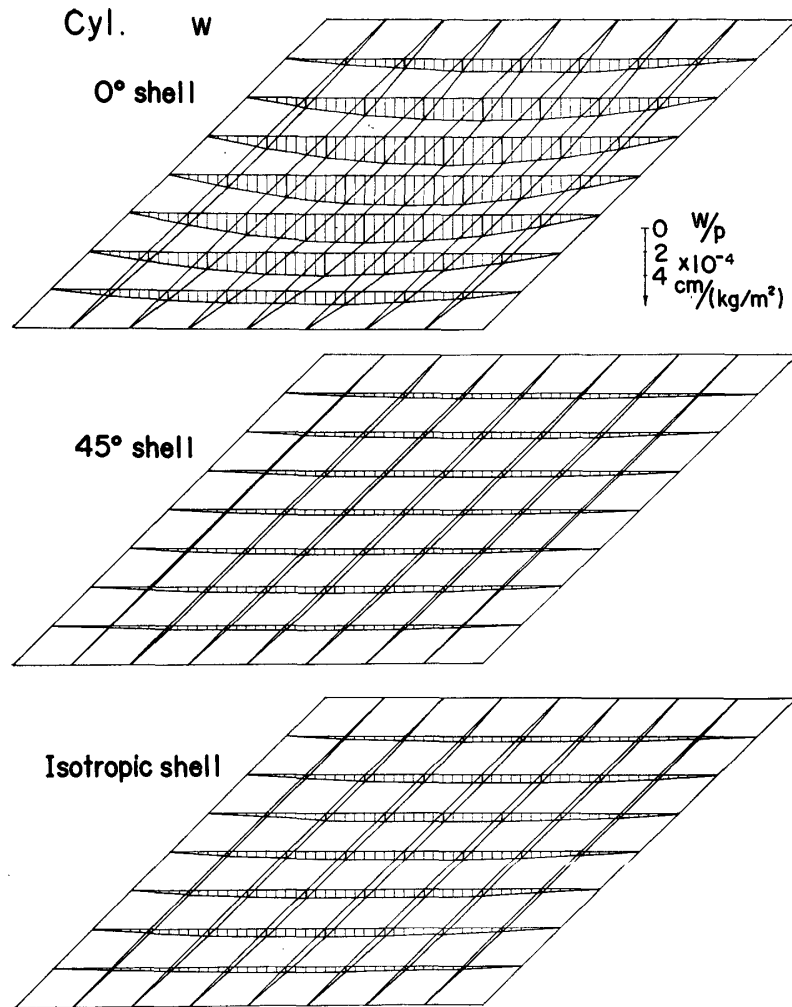


Fig. 15. The distribution of the deflection of the cylindrical shells ( $k_x=0.01$  or rise/span=0.075) under uniform pressure. See \* and \*\* in Fig. 7. The moduli of elasticity of the isotropic shell are shown in Table 2-F.

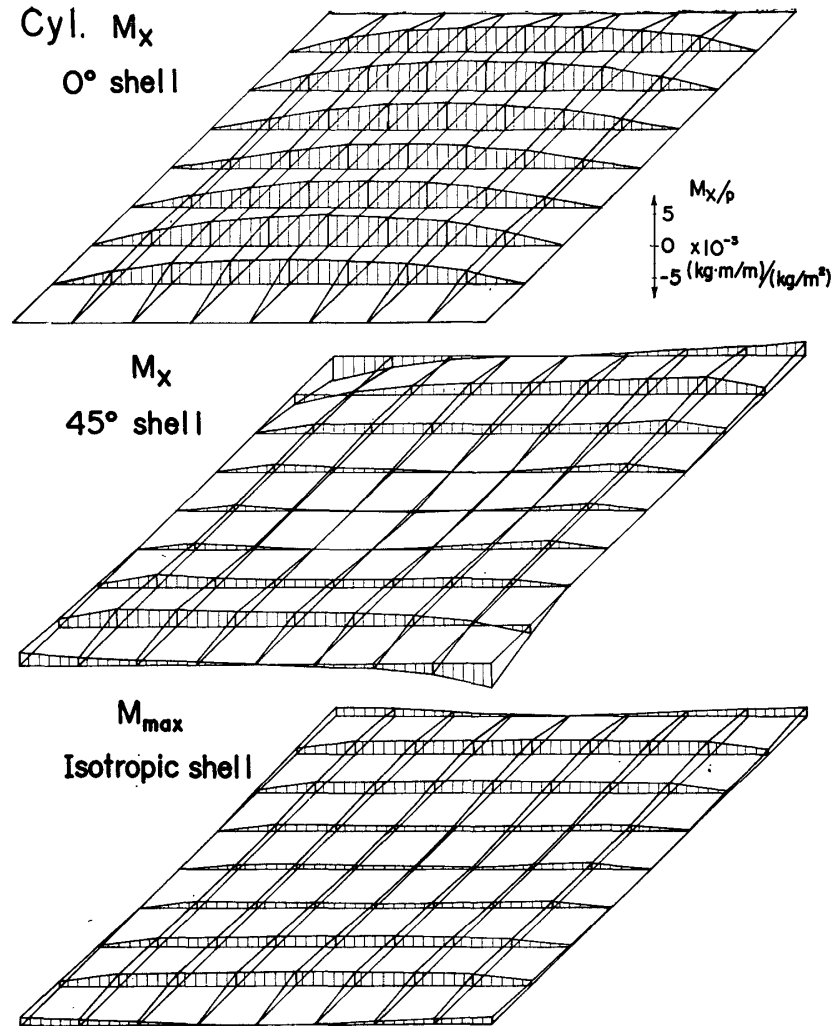


Fig. 16. The distribution of the bending moment of the cylindrical shells under uniform pressure. These are the same shells as those shown in Fig. 15.  $M_{max}$  denotes the maximum bending moment. When the case \*\*\*\* in Table 2, the unit of the scale is  $\times 10^{-1} (\text{kg}\cdot\text{m}/\text{m})/(\text{kg}/\text{m}^2)$ .

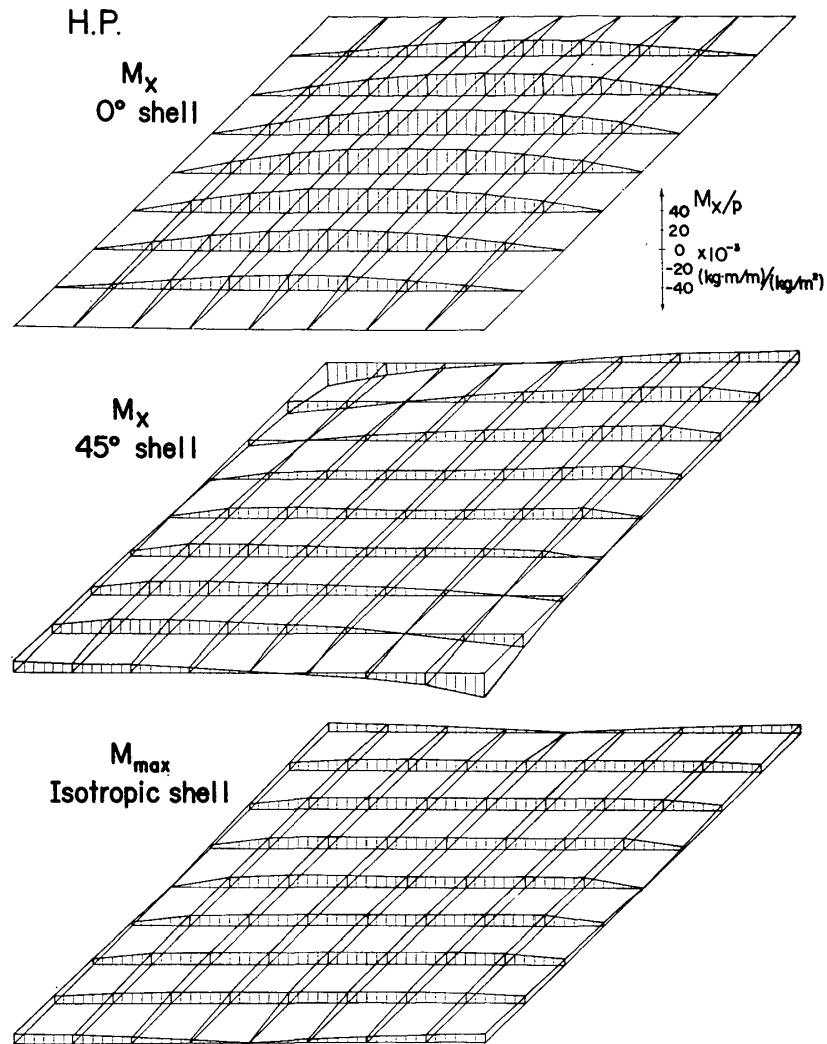


Fig. 17. The distribution of the bending moments of the H. P. shells ( $k_{xy}=0.005$ ) under uniform pressure. See \* in Fig. 7. The moduli of elasticity of the isotropic shell are shown in Table 2-F

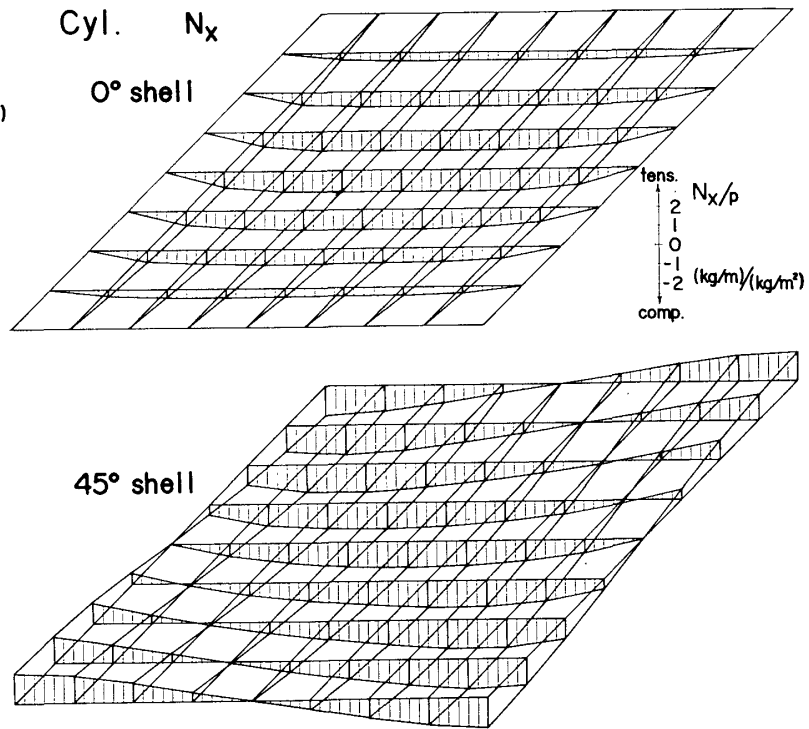


Fig. 18. The distribution of the membrane force  $N_x$  of the orthotropic cylindrical shells under uniform pressure. These are the same shells as those shown in Fig. 15. See \* in Fig. 9.

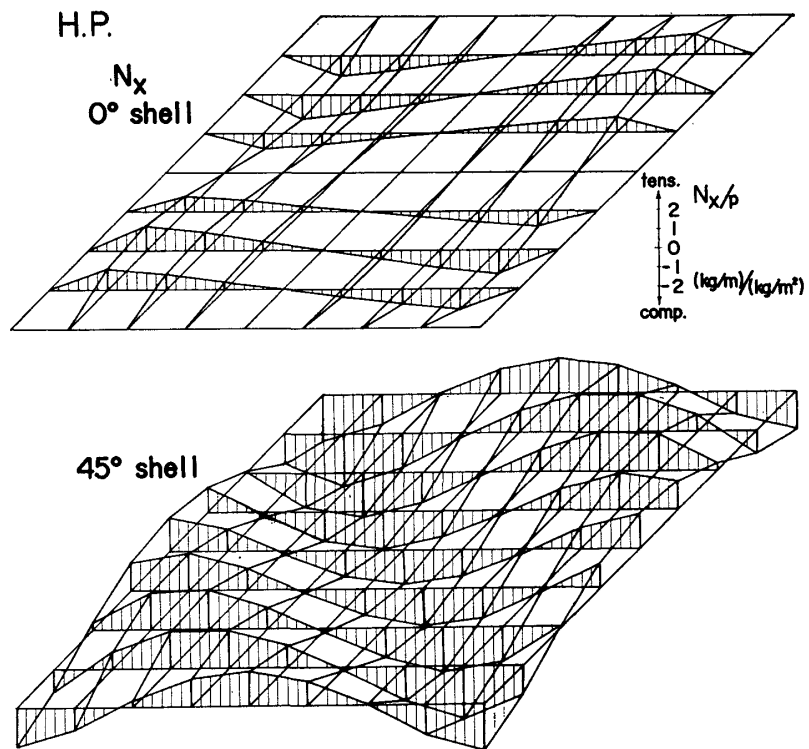


Fig. 19. The distribution of the membrane force  $N_x$  of the orthotropic cylindrical shells under uniform pressure. These are the same shells as those shown in Fig. 17. See \* in Fig. 9.

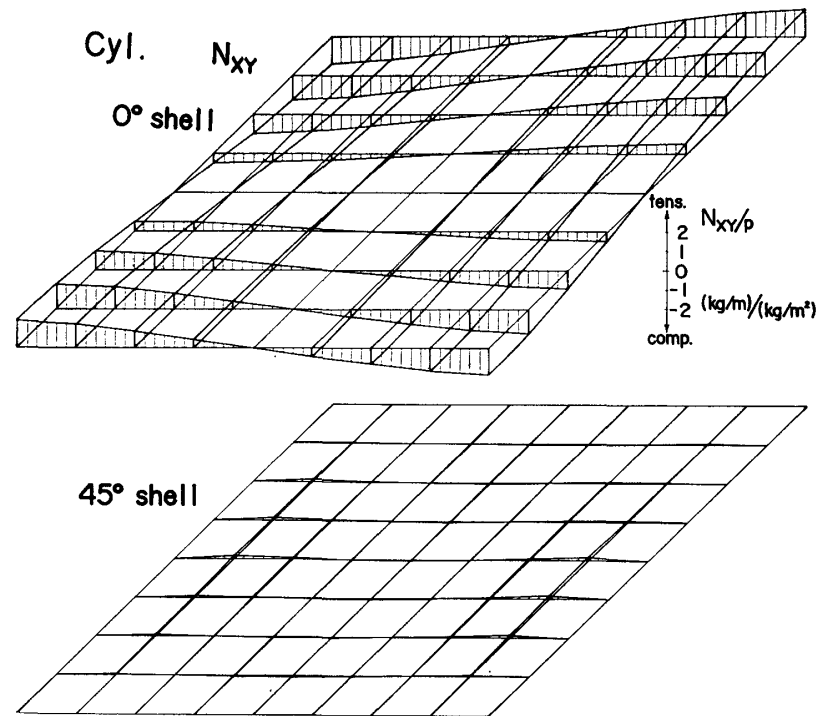


Fig. 20. The distribution of the membrane shearing force  $N_{xy}$  of the orthotropic cylindrical shells under uniform pressure. These are the same shells as those shown in Fig. 15. See \* in Fig. 9.



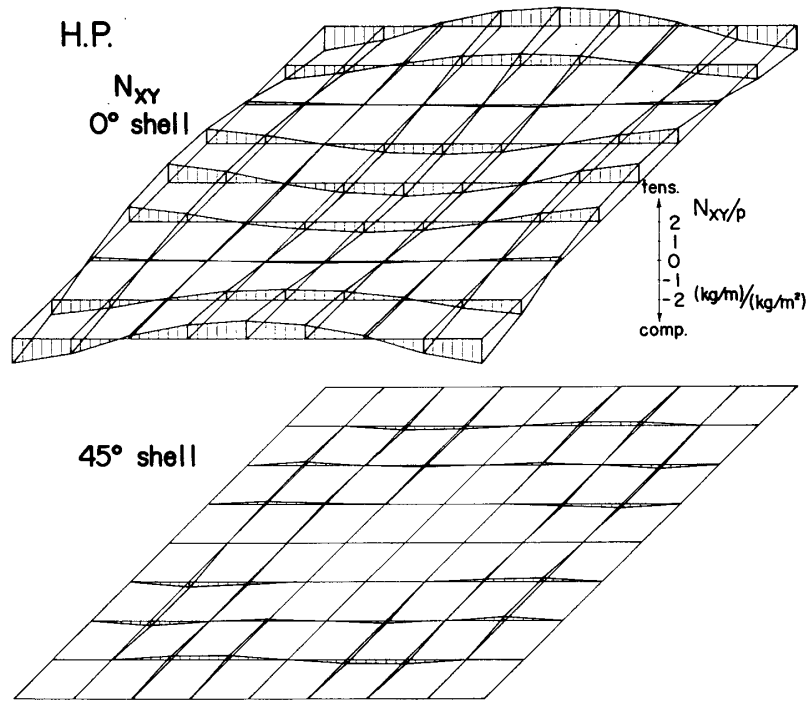


Fig. 21. The distribution of the membrane shearing force  $N_{XY}$  of the orthotropic H. P. shells under uniform pressure. These are the same shells as those shown in Fig. 17. See \* in Fig. 9.

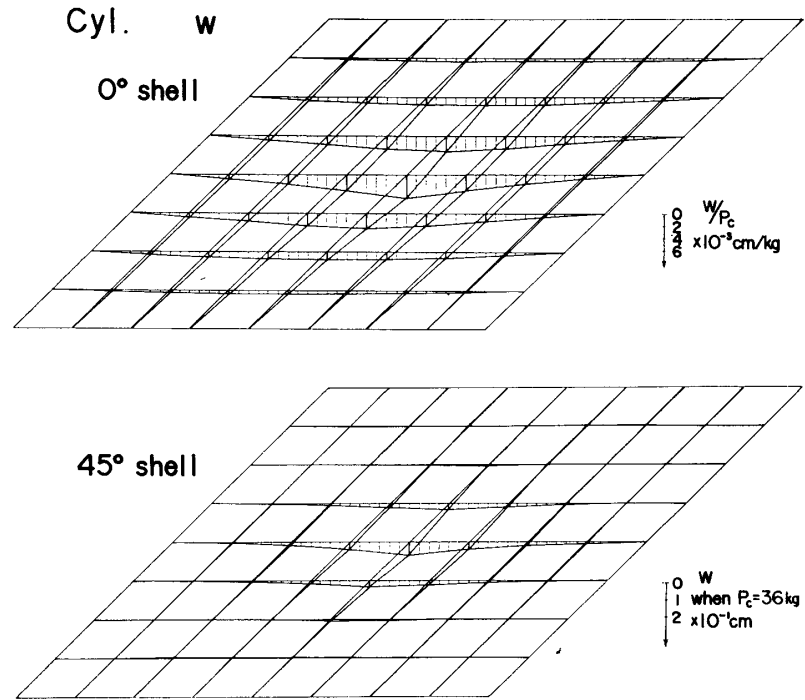


Fig. 22. The distribution of the deflection of the orthotropic cylindrical shells ( $k_x=0.01$  or rise/span=0.075) under a central concentrated load  $P_c$ . See \* in Fig. 7 and Table 4.

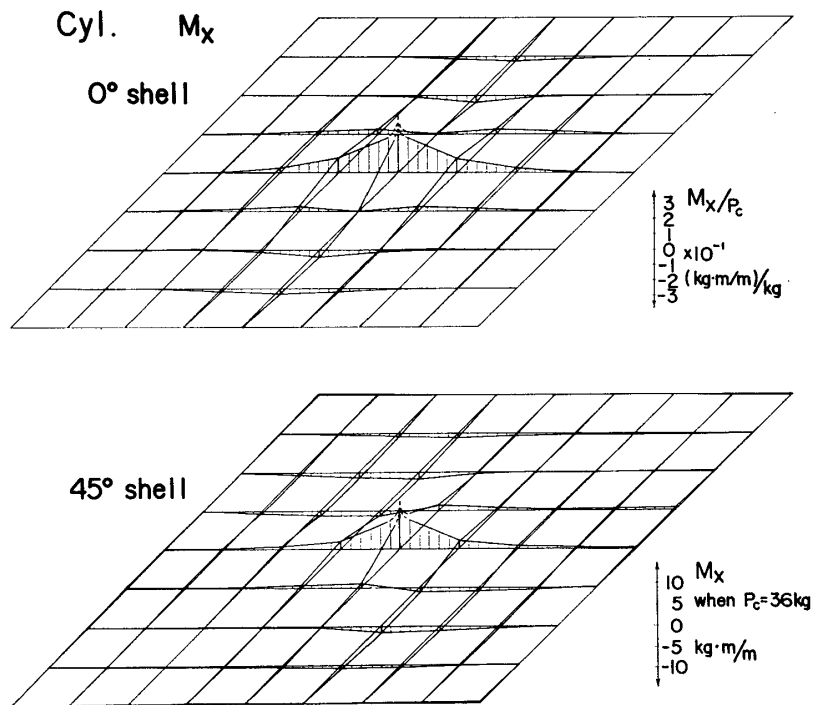


Fig. 23. The distribution of the bending moment  $M_x$  of the orthotropic cylindrical shells under a central concentrated load  $P_c$ . See Fig. 22.

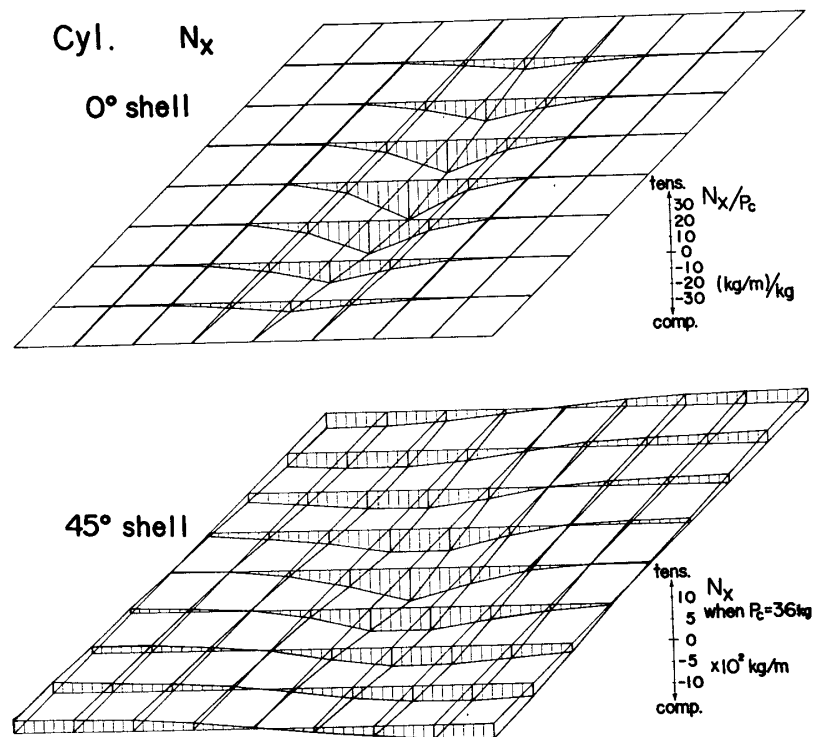


Fig. 24. The distribution of the membrane force  $N_x$  of the orthotropic cylindrical shells under a central concentrated load  $P_c$ . See Fig. 22.

the  $0^\circ$  shell. And the curves are depressed near the central parts. The depression of the  $45^\circ$  shell and that of the isotropic shell are much larger than that of the  $0^\circ$  shell. Particularly, the bending moment value of the  $45^\circ$  shell becomes negative near the center (cf. Fig. 13). The bending moment curves on the edges of the  $45^\circ$  shell are complicated, and two of the diagonally opposite corners have the negative bending moment value as shown in Fig. 16. The similar phenomenon is also observed in the H. P.  $45^\circ$  shell (see Fig. 17). The central depressions in the H. P. ( $45^\circ$  and isotropic) shells are smaller than those of the cylindrical shells. The bending moment value of the H. P. shells are about 7 times as large as that of the cylindrical shells as shown by the scales of Figs. 16 and 17.

The figures of the distribution of the bending moment perpendicular to the elastic principal axis are omitted. The values are about half of  $M_x$ , and the distribution curves are similar to those of  $M_x$ .

The figures of  $M_{xy}$  (the torsion moment parallel to the elastic principal axis) are also omitted, because the values of the orthotropic shells are much smaller than those of  $M_x$ . The  $M_{xy}$  of the  $45^\circ$  shell is nearly equal to zero.

#### *Membrane Forces*

The distribution curves of the membrane forces ( $N_x, N_{xy}$ ) of the H. P. shells are more complicated than those of the cylindrical shells (see Figs. 18 and 19).

The shear membrane forces of the  $45^\circ$  shells are much smaller than those of  $0^\circ$  (see Figs. 20 and 21). This is an advantage of the  $45^\circ$  shells.

The average of the membrane forces of the H. P. shells are nearly equal to or a little larger than those of the cylindrical shells, but the moments of the H. P. shells are much larger than those of the cylindrical shells. This is a disadvantage of the roller-supported H. P. shells, and an advantage of the cylindrical shells.

### **5. Central Concentrated Load**

The distributions of "the deflections, the bending moments and the membrane forces" of the cylindrical shells "under a concentrated load" are shown in Figs. 22~24. And the central deflection of "the plates, the cylindrical shells and the H. P. shells" are shown in Table 4. The deflection of the plates and the H. P. shells under the concentrated load, which is equal to the total of the uniform pressure, is "about 3 times" as large as that under uniform pressure. With respect to the cylindrical shells, the ratio becomes larger as the curvature increases. And when  $k_x$  equals to 0.01, the ratio is about 4.5 for the  $0^\circ$  shell and about 14 for  $45^\circ$  shell. Nevertheless the deflection of the  $45^\circ$  shell is much smaller than that of  $0^\circ$  shell (about 60% of that of  $0^\circ$  shell).

Table 4. Central deflection of the shells and plates under a central concentrated load\*:  $w_c/p$  (mm/36kg).

$\theta$	Plate	Cyl. $k_x=0.005$	Cyl. $k_x=0.01$	H. P. $k_{xy}=0.005$
0°	5.828	2.884	1.368	5.009
30°	4.201	1.712	0.894	3.236
45°	3.821	1.372	0.786	2.672
90°	5.828	2.935	1.474	5.009

Ratio of the central deflection of the shells and plates "under a central concentrated load" to that of "under uniform pressure"\*:  $w_c/w_u$ .

$\theta$	Plate	Cyl. $k_x=0.005$	Cyl. $k_x=0.01$	H. P. $k_{xy}=0.005$
0°	2.94	3.37	4.43	2.94
30°	3.13	5.08	7.98	3.11
45°	3.21	5.49	13.87	3.17
90°	2.94	3.45	4.96	2.94

\* The moduli of elasticity are the same as those of C in Table 2. The dimension is 60cm×60cm×0.9cm. The concentrated load (36kg) is equal to the total of the uniform pressure (100kg/m<sup>2</sup>).

The distribution curves of the bending moments have steep ascent near the center of the shells (compare Fig. 23 with Fig. 16). And the bending moments at the center are infinite, so the center *i. e.* the loaded point is a singular point for the elastic analysis.

The distribution curves of the membrane force  $N_x$  have the mountain range which runs parallel to each principal elastic axis as shown in the both figures of 0° shell and 45° shell (compare Fig. 24 with Fig. 18 with consideration of the scales). The distribution curves of  $N_y$  of "0° shell" have not such a mountain range but those of  $N_y$  of "45° shell" have a similar mountain range which runs diagonally (parallel to  $Y$  axis).

#### Acknowledgement

The present numerical works were carried out by the computer FACOM 230-60 in Kyoto Univ. The authors wish to thank Mrs. M. Katsuyama for her helpful drawing of the figures from the computation results.

#### Literature

- 1) L. O. KERESZTESY, "Timber Shells" (1970) Timber Research and Development Association.
- 2) K. HOFFMAN and H. GRIESE, "Building with Wood", p 113 (1969) FREDERICK A. Praeger, Publishers, New York.

MASUDA, MAKU : Plywood Shallow Shells (I)

- 3) S. A. AMBARTSUMYAN, "Theory of Anisotropic Shells" (1961) NASA Technical Translation TTF-118.
- 4) K. APELAND, Civil Engineering and Building Construction Series No. 22, Acta Polytechnica Scandinavica (1963).
- 5) J. R. GOODMAN, Forest Products J., 16, No. 10, 49 (1966).
- 6) J. R. GOODMAN, "Timber Shell Structures" Fellowship Report to National Lumber Manufacturers Association (1964).
- 7) R. F. S. HEARMON, "The Elasticity of Wood and Plywood" p 25 (1948) His Majesty's Stationery Office, London.
- 8) R. F. S. HEARMON, "An Introduction to Applied Anisotropic Elasticity" (1961) Oxford University Press.
- 9) M. MASUDA, H. SASAKI and T. MAKU, Wood Research, No. 47, 12 (1969).
- 10) M. MASUDA and T. MAKU, J. of the Society of Materials Science, Japan, 20, 1213 (1971).